Peroxidase Activity in Prostaglandin Endoperoxide H Synthase-1 Occurs with a Neutral Histidine Proximal Heme Ligand†

Steve A. Seibold,‡,§ Jose F. Cerda,‡ Anne M. Mulichak,§ Inseok Song,|| R. Michael Garavito,§ Toshiya Arakawa, William L. Smith,§ and Gerald T. Babcock*,‡

Department of Biochemistry, Department of Chemistry and the LASER Laboratory, Michigan State University, East Lansing, Michigan 48824

Received February 2, 2000; Revised Manuscript Received March 28, 2000

ABSTRACT: Prostaglandin endoperoxide H synthases-1 and -2 (PGHS-1 and -2) convert arachidonic acid to prostaglandin H_2 (PGH_2), the committed step in prostaglandin and thromboxane formation. Interaction of peroxides with the heme sites in PGHSs generates a tyrosyl radical that catalyzes subsequent cyclooxygenase chemistry. To study the peroxidase reaction of ovine oPGHS-1, we combined spectroscopic and directed mutagenesis data with X-ray crystallographic refinement of the heme site. Optical and Raman spectroscopy of oxidized oPGHS-1 indicate that its heme iron (Fe^{3+}) exists exclusively as a high-spin, six-coordinate species in the holoenzyme and in heme-reconstituted apoenzyme. The sixth ligand is most likely water. The cyanide complex of oxidized oPGHS-1 has a six-coordinate, low-spin ferric iron with a v[Fe−CN] frequency at 445 cm^{-1}; a monotonic sensitivity to cyanide isotopomers that indicates the Fe−CN adduct has a linear geometry. The ferrous iron in reduced oPGHS-1 adopts a high-spin, five-coordinate state that is converted to a six-coordinate, low-spin geometry by CO. The low-frequency Raman spectrum of reduced oPGHS-1 reveals two v[Fe−His] frequencies at 206 and 222 cm^{-1}. These vibrations, which disappear upon addition of CO, are consistent with a neutral histidine (His388) as the proximal heme ligand. The refined crystal structure shows that there is a water molecule located between His388 and Tyr504 that can hydrogen bond to both residues. However, substitution of Tyr504 with alanine yields a mutant having 46% of the peroxidase activity of native oPGHS-1, establishing that bonding of Tyr504 to this water is not critical for catalysis. Collectively, our results show that the proximal histidine ligand in oPGHS-1 is electrostatically neutral. Thus, in contrast to most other peroxidases, a strongly basic proximal ligand is not necessary for peroxidase catalysis by oPGHS-1.

The formation of PGH_2 from arachidonate catalyzed by prostaglandin endoperoxide H synthases-1 and -2 (PGHS-1 and -2)[1] is the committed step in prostaglandin and thromboxane biosynthesis. PGHSs catalyze both the conversion of arachidonic acid and two molecules of oxygen to prostaglandin G_2 (PGG_2) and a subsequent two electron reduction of the 15-hydroperoxyl group of PGG_2 to PGH_2 (*1*−*4*). These two reactions, the cyclooxygenase and peroxidase reactions, respectively, occur at physically distinct sites within the enzyme (*5*−*8*). The cyclooxygenase activity of PGHSs is important pharmacologically because both isoforms are major targets of aspirin and other nonsteroidal antiinflammatory drugs (*9*, *10*).

Scheme 1: Peroxidase Cycle of PGHS-1[a]

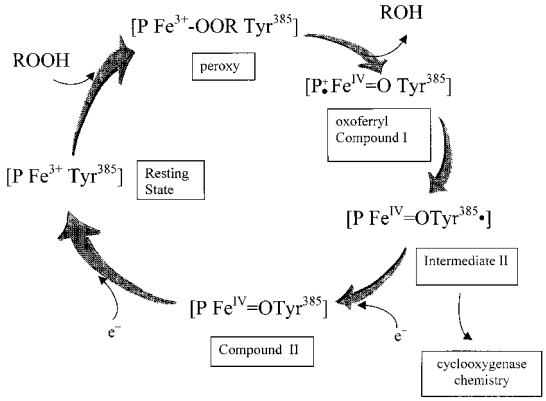

[a] Proposed intermediates involved in the production of the tyrosine radical and the subsequent reduction of the enzyme to the resting state [PFe^{3+}Tyr], where P represents protporphyrin IX. After the binding of substrate to form the peroxy compound, the resting enzyme is oxidized by 2 electron equiv with the concommitant splitting of molecular oxygen. This oxoferryl species (compound I) is then reduced by the Try^{385} to generate the intermediate 2 species. The subsequent Try^{385} radical is thought to initiate the cyclooxygenase activity of the enzyme. The enzyme can then be reduced to resting state by the addition of two electron equivalents.

The peroxidase and cyclooxygenase activities of PGHSs are mechanistically interrelated (*4*, *11*; see Scheme 1). The

† This work supported by NIH Grants R01 HL56773 (R.M.G.) and P01 GM57323 (G.T.B., R.M.G., and W.L.S.).

* To whom correspondence should be addressed. E-mail: Babcock@cem.msu.edu.

‡ Department of Chemistry and the LASER laboratory.

§ Department of Biochemistry, Michigan State University.

|| University of Seoul, Department of Life Science, Seoul Korea.

[1] Abbreviations: PGHSs, prostaglandin endoperoxide H synthases; oPGHS-1, ovine PGHS-1; PBS, phosphate-buffered saline; DMEM, Dulbecco's modified Eagle's medium. HRP, horseradish peroxidase; Mb, myoglobin, LPO, lactoperoxidase; CIP, *Coprinus cinereus* peroxidase; CCP, yeast cytochrome *c* peroxidase; $PPFe^{3+}$-Im_2, Protoporphyrin IX (Fe^{3+})bis-imidazole complex; CN, cyanide; N_3, azide; CO, carbon monoxide.

10.1021/bi0002333 CCC: $19.00
Published on Web 05/10/2000

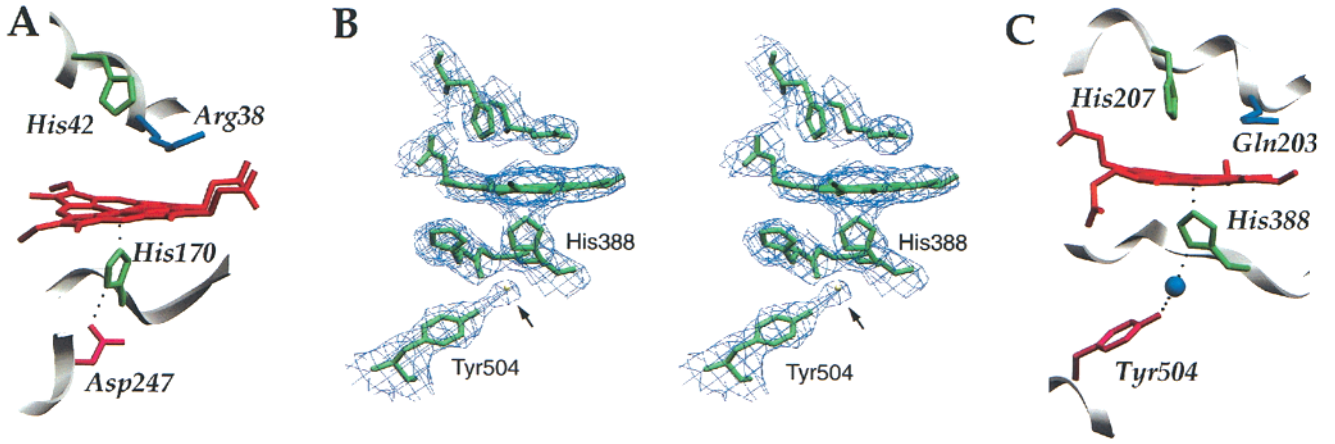

FIGURE 1: Comparison of the proximal and distal sites of horseradish peroxidase and oPGHS-1. Figures are derived from the crystal structures of (A) horseradish peroxidase (35) and (C) the refined crystal structure of oPGHS-1 with its electron density map shown in panel B. The proximal histidine of horseradish peroxiase is hydrogen bonded to an adjacent Asp247 while the equivalent position in oPGHS-1 is a water molecule, shown as a ball, which intervenes between the Nδ of His388 and the phenolic oxygen of Tyr504.

heme group at the peroxidase active site is oxidized by an alkyl hydroperoxide (e.g., PGG_2) to yield an alcohol and a Compound I peroxidase intermediate having an oxoferryl group and a heme radical cation (*11*−*14*). Compound I can undergo one-electron reduction by either of two routes (*15*). Using an exogenous electron donor, Compound I can be reduced to a typical Compound II peroxidase intermediate. Alternatively, Tyr385 can act as an intramolecular electron donor to form Intermediate II, which consists of a tyrosyl radical and an oxyferryl heme. The tyrosyl radical (Tyr385$^{\bullet}$) is the species that abstracts the 13pro*S* hydrogen from arachidonate to initiate the cyclooxygenase reaction. Thus, the cyclooxygenase reaction depends on the initial oxidation of the heme group at the peroxidase active site. In contrast, the peroxidase itself can function in the absence of cyclooxygenase catalysis (*15*, *16*).

The peroxidase activity of PGHSs has structural, kinetic and spectral properties similar to other peroxidases (*1*−*4*); indeed, the structure of PGHS is very closely related to that of myeloperoxidase (*6*−*8*). His388 of ovine (o) PGHS-1 is the proximal histidine residue coordinating the heme iron. His207 is the distal histidine and Gln203 is in the distal pocket at a location corresponding to the catalytically relevant distal Arg of other peroxidases (Figure 1). According to the widely accepted "push−pull" mechanism used to explain peroxidase catalysis, the proximal and distal amino acids facilitate the heterolytic cleavage of the oxygen−oxygen bond of substrate peroxide (*17*−*19*). Key to this mechanism is the notion that the proximal ligand is strongly basic. This may occur either because of its intrinsic chemistry (phenolate, cysteinate) or, in the case of a proximal histidine, because secondary interactions impart significant histidinate character to this residue.

Although the push−pull mechanism has been used extensively in the discussion of peroxidase catalysis, increasingly, there have been apparent exceptions to this model. For example, the proximal histidine in cytochrome *c* peroxidase can be substituted mutagenetically with glutamine without significant impact on Compound I formation (*20*). Some other exceptions are discussed by Poulos, Goodin and Smulevich (*17*, *21*, *22*). Most recently, Franzen et al. (*23*) have reported that a neutral histidine, rather than the more basic histidinate, occurs in two marine worm peroxidases and Hager and co-workers have succeeded in replacing the proximal cysteinate in chloroperoxidases with histidine without loss of activity (*24*).

The goal of the studies reported here is to investigate properties of the peroxidase heme binding pocket of oPGHS-1, particularly the chemical nature of the interaction between the heme group and the proximal histidine, His388. The results of previous studies of this topic have been somewhat puzzling. Room-temperature magnetic circular dichroism studies with the resting, ferric enzyme suggest that a subpopulation of the enzyme (20%) can exist in a low-spin, six-coordinate state (*25*); this type of coordination state is unusual for peroxidases. Moreover, UV−vis absorption data have been interpreted to indicate that ferrous heme in the reduced enzyme at room-temperature equilibrates to a six-coordinate, low-spin state (*26*). We have used a combination of crystallographic data refinement, UV−vis, resonance Raman, and EPR spectroscopies along with mutational analysis of oPGHS-1 to determine the spin-states of the oxidized and reduced forms of the enzyme and to delineate the interaction between the heme iron and the proximal histidine. We have found that homogeneous spectral behavior is observed for both oxidized and reduced oPGHS-1 following heme reconstitution and that the distal pocket of native oPGHS-1 is relatively unconstrained. Most importantly, we have determined that the interaction between the heme iron and proximal histidine involves a neutral histidine. Thus, in contrast to most peroxidases, electron donation provided by a strong proximal base is not essential for oPGHS-1 peroxidase catalysis.

MATERIAL AND METHODS

Enzyme Preparations and Chemicals. oPGHS-1 was purified to homogeneity from sheep seminal vesicle microsomes using a modified isolation technique derived from Harlan et al. (*27*) where *N*-decyl-heptaethyleneglycol monoether ($C_{10}E_7$; Fluka) was utilized as the detergent for enzyme isolation and purification (M. Harris and M. J. Theisen, personal communication). Typically, the isolated enzyme was concentrated and resuspended in 50 mM phosphate buffer, pH 7 in the presence of 0.1% $C_{10}E_7$. Although oPGHS-1 isolated by this procedure was 50% or greater holoenzyme

upon isolation, it was reconstituted with heme (protein:heme was 1:0.5−1.0) to generate heme-reconstituted enzyme. The enzyme/heme solution, in the presence of excess flurbiprofen (80 μM or greater), was then incubated with DEAE cellulose for 30 min at room temperature, using gentle agitation, and then filtered through a macrofiltration centrifugation tube (Altech) to separate the free porphyrin-bound-DEAE mesh from the holo-oPGHS-1. The protein solutions were then examined by using an AVIV 14DS UV−vis optical absorption spectrometer and resonance Raman spectroscopy. The final concentration of reconstituted enzyme for our experiments was typically 30−40 μM. All UV−vis absorption studies for reconstitution were done using a value of ϵ = 165 000 cm^{-1} M^{-1} at a λ_{max} = 412 nm (*28*).

Potassium cyanide was purchased from Sigma, and the cyanide isotopes were from Cambridge Isotopes, Inc. The cyanide complexes of oPGHS-1 were prepared by the addition of aliquots from stock solutions of 100 mM cyanide at pH 11.5 to the enzyme in 40 mM-Tris buffer at pH 7. Reduced enzyme was generated by placing the protein under an argon gas atmosphere in a spinning cell and adding an aliquot of dithionite in deaerated buffer. CO and its isotopes were obtained from Icon: Stable Isotopes, Inc. The ferrous CO-oPGHS-1 adducts were prepared by exposing the reduced enzyme to a CO atmosphere under anaerobic conditions.

Preparation of Y504A oPGHS-1. Y504A oPGHS-1 was prepared by starting with M13mp19-oPGHS-1, which contains a 2.3 kb *Sal*I fragment encoding native oPGHS-1 (*29*, *30*) by using a BioRad Muta-Gene kit and the manufacturer's protocol. The oligonucleotide used for mutagenesis was 5′-^{1594}GATGCTTTGGAATTCGCCCCGGGGCTACTTCT-TG^{1627}-3′. Single-stranded phage samples were sequenced with Sequenase (ver. 2.0, U.S. Biochemical Corp.) and the protocol described by the manufacturer. The replicative form of M13mp19-oPGHS-1 containing the Y504A mutation was prepared from phage cultures, digested with *Sal*I, isolated by gel electrophoresis and electroluted into dialysis tubing using standard protocols. The resulting 2.3 kb oPGHS-1 cDNA fragment was purified and subcloned into pSVT7, followed by digestion with *PstI* to verify the orientation of the insert (*29*−*31*). Plasmids used for transfection were purified by CsCl gradient ultracentrifugation, and the mutation was reconfirmed by double-stranded sequencing of the pSVT7 construct as described above.

Transfection of COS-1 Cells with Recombinant oPGHS-1. COS-1 cells (ATTC CRL-1650) were grown in DMEM containing 8% calf serum and 2% fetal bovine serum until near confluence (~3 × 10^6 cells/10 cm dish) (*29*−*31*). Cells were then transfected with a pSVT7 plasmid containing cDNA encoding native or Y504A oPGHS-1 by using the DEAE dextran/chloroquine transfection method as reported previously (*29*−*31*). Forty hours following transfection, cells were harvested in cold phosphate-buffered saline (PBS), collected by centrifugation and resuspended in 0.1 M Tris-HCl, pH 7.5. Sham-transfected cells were collected in an identical manner. Microsomes were prepared from transfected cells and used for cyclooxygenase and peroxidase assays as described in detail previously (*32*).

Spectroscopic Measurements. Resonance Raman scattering was detected with a spectrometer (Spex 1877 Triplemate) by using a liquid nitrogen cooled CCD detector (EG&G OMA 4, model 1530-CUV-1024S). The samples were placed in a spinning cell at room temperature or cooled to ~10 °C. The Raman spectra of the oxidized and cyanoferric PGHS-1 complexes were obtained by using the 413.1 nm excitation line of a Kr^+ laser (Coherent K-90) laser. To obtain Raman spectra of the ferrous and of the Fe-CO oPGHS-1, a dye laser (Coherent CR599) with Stilbene 420 as the dye was pumped by an Ar^+ laser (Coherent Innova 200) to generate the appropriate excitation line. Enzyme integrity before and after exposure to the laser was determined by optical spectroscopy. Reconstituted and unreconstituted oPGHS-1 were prepared and their EPR spectra were recorded at liquid helium temperatures using a Bruker 300E X band spectrometer equipped with a TE_{102} cavity and an Oxford ESR-9 cryostat.

oPGHS-1 Structural Refinement. For the improved structural analysis, the previously published crystal structure of oPGHS-1 complexed with flurbiprofen (*6*) was extended to a higher resolution and refined. Phases for the X-ray data collected by Picot et al. (*6*) were calculated and refined for shells of resolution from 3.5 Å to 3.1 Å resolution with X-PLOR. Noncrystallographic symmetry restraints between the two molecules of the oPGHS-1 dimer were utilized. As refinement progressed, data from 3.0 Å were included with bulk solvent correction and restrained individual *B*-factor refinement was performed. In the final stages of refinement, a modest number (130) of water molecules were added at positions having high (3σ) peaks in $F_o - F_c$ electron density maps and good hydrogen-bonding geometry with appropriate protein atoms. The final model, with an average *B*-factor of 22 $Å^2$, has an *R*-factor of 0.197 (R_{free} = 0.230). Atomic coordinates have been deposited in the Protein Data Bank (entry 1CQE).

RESULTS

Crystal Structure Refinement of oPGHS-1. Most aspects of the oPGHS-1 structure relevant to catalytic function have been reported elsewhere (*6*). Nearly all of the water molecules included in the extended refinement of the flurbiprofen complex are buried within the protein structure or fill deep pockets in the protein surface. In one case, a series of five buried water molecules form a solvent channel in each monomer which extend perpendicularly from the end of the cyclooxygenase channel near Gly533 and open into the bottom of a second deep channel coincident with the dimer 2-fold rotation axis. Of particular relevance to the peroxidase reaction is an isolated and buried water molecule which hydrogen bonds (2.7 Å) to the backside of the proximal His388 side chain via the Nδ atom (Figure. 1B). This solvent position, also within hydrogen-bonding distance (2.8 Å) of the adjacent Tyr504 side-chain phenolic group, shows good electron density in both PGHS monomers, and refinement yields *B*-factors of 26 and 21 $Å^2$ for the two sites, values similar to the average for the protein structure. Interestingly, this water molecule assumes a position similar to Asp or Asn side chains that form a hydrogen bond with the proximal histidine in the structurally homologous myeloperoxidase, lignin peroxidase, horseradish peroxidase (Figure 1A) and cytochrome *c* peroxidase (*33*−*38*). In the oPGHS-1 structure, these side-chain−side-chain interactions, which are characteristic of other peroxidases, are not conserved, as a valine is found at the position corresponding

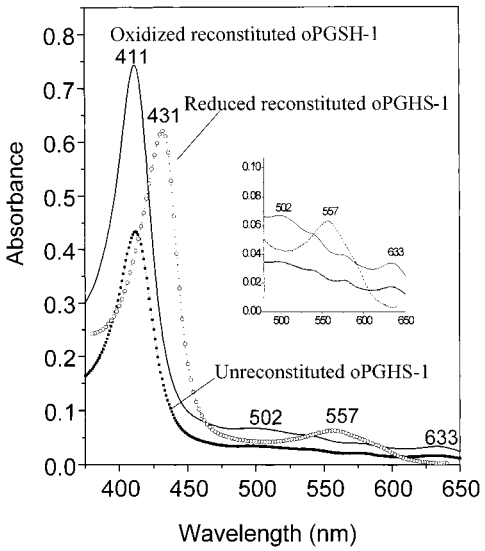

FIGURE 2: UV−vis absorption spectra of unreconstituted oxidized oPGHS-1 (■), oxidized reconstituted oPGHS-1 (solid line) and reduced reconstituted oPGHS-1 (○). Unreconstituted holo-oPGHS-1 (14 μM) was exposed to 28 μM hematin and the unbound heme was removed as stated in the Material and Methods. The final concentration of the reconstituted oPGHS-1 was 25 μM. The reconstituted enzyme was subsequently reduced with dithionite in 50 mM phosphate buffer pH 7, and the UV−vis absorption spectrum was determined.

to the Asp or Asn in related peroxidases. A solvent-mediated interaction between the proximal histidine His388 and Tyr504 appears to substitute for the direct side chain interactions of other peroxidases (Figure. 1C). Some electron density has also been observed near the sixth (distal) coordination position of the heme iron of oPGHS-1, but is not seen in all maps at this resolution. Thus, a water molecule as a sixth iron ligand is possible, but not confirmed. Moreover, there is no evidence for any direct interactions on the distal heme face between the heme iron and either His207 or Gln203, the two residues that are likely to be involved in the catalytic mechanism in PGHSs. Therefore, the refined crystal structure of oPGHS provides additional insights into the positions of water at the proximal and distal heme positions. To obtain more quantitative information about the physical and chemical environment of the heme, we performed a variety of spectroscopic measurements on oPGHS-1 in the presence and absence of exogenous heme ligands.

Spectroscopic Characterization of Ferric oPGHS-1 Using Native and Heme-Reconstituted Protein. The heme group of oPGHS-1 is relatively loosely bound to the enzyme ($K_d \approx 1$ μM) so that oPGHS-1 has been purified primarily as apoenzyme with earlier methods (*39*−*41*). Although our preparation significantly improved the yield of holoenzyme (see Material and Methods), we have also used oPGHS-1 that was reconstituted with heme for most of our spectral investigations. Heme reconstitution has been shown to produce heterogeneous populations in myoglobin (*42*) and leads to anomalies in the resonance Raman spectra of guanylate cyclase (*43*). Addition of suprastoichiometric levels of heme to oPGHS-1 yields a preparation with mixture of spin states (*26*). Accordingly, we first determined whether there were differences between the spectra of oPGHS-1 unreconstituted and oPGHS-1 heme-reconstituted with approximately stoichiometric amounts of heme.

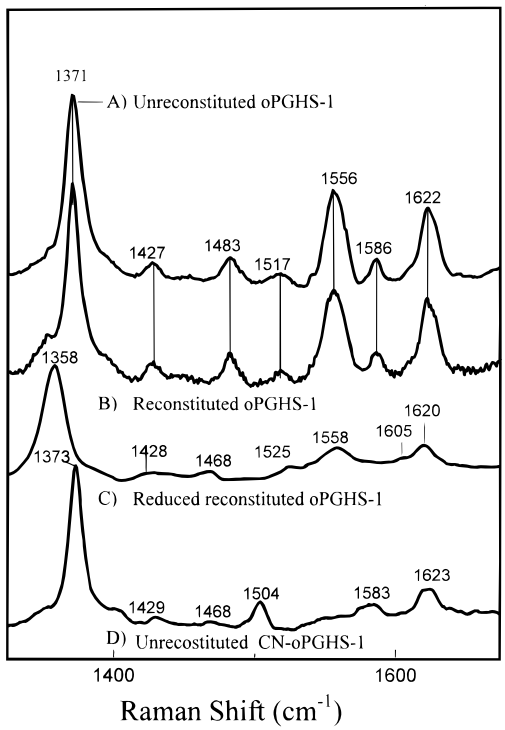

FIGURE 3: High-frequency resonance Raman spectra of (A) 35 μM oxidized unreconstituted oPGHS-1, (B) 42 μM oxidized reconstituted holo-oPGHS-1, (C) reconstituted enzyme, (B) reduced with dithionite, (D) 25 μM unreconstituted oPGHS-1 exposed to 10 mM CN to generate the CN-oPGHS-1 adduct. Panels A, B, and D were obtained using the 413.1 nm excitation line, while panel C was obtained utilizing the 433 nm line from a stilbene3 dye laser. Panels A and D were at room temperature at pH 7.0 in 40 mM Tris-HCl/Bis-Tris-HCl buffer, with 0.1% $C_{10}E_7$ while B and C were at ~10° C at pH 7 in 50 mM potassium phosphate buffer with 0.1% $C_{10}E_7$.

For the oxidized enzyme, the UV−vis (Figure 2), resonance Raman (Figure 3) and EPR spectra (not shown) of both unreconstituted- and heme-reconstituted oPGHS-1 were essentially identical. The Raman spectra in Figure 3 indicate that oPGHS-1 in its oxidized resting state exists solely as a high-spin, six-coordinate structure (Table 1). The vibrational data indicate the absence of a high-spin, five-coordinate structure, in agreement with Tsai et al. (*44*) and Gaspard et al. (*26*). There were no signals in the EPR spectra recorded at liquid helium temperatures that were typical of the population of low-spin, six-coordinate structures observed previously (*25*). We conclude that both unreconstituted- and heme-reconstituted oPGHS-1 in its resting, ferric state exists as a homogeneous six-coordinate, high-spin population with water as the sixth ligand. The optical and Raman data remove the ambiguity in the crystallographic data discussed above by showing that indeed water occurs as the sixth ligand to the heme iron in the resting enzyme.

For the reduced enzyme, we observed similar results for the unreconstituted- and heme-reconstituted protein. There were no significant optical or Raman differences between the preparations (not shown). Thus, heme reconstitution using approximately stoichiometric amounts of heme reconstitutes the native enzyme in both its oxidized and reduced states.

Cyanide-Adduct of Ferric oPGHS-1. Resonance Raman spectra of the cyanide adduct of oxidized oPGHS-1 were collected at pH 7 using excitation from the 413 nm line. The high-frequency spectrum in Figure 3 of the CN-oPGHS complex indicates an oxidized, low-spin, six-coordinate

Table 1: Comparison of High Mode Number Raman Bands Obtained for oPGHS-1 with Those of Other Heme Proteins and Model Complexes[a]

frequency	oPGHS-1 (Fe^{3+})	F−HRP (Fe^{3+})	Mb (Fe^{3+})	CCP (Fe^{3+})	catalase (Fe^{3+})	CIP (Fe^{3+})	$PPFe^{3+}$-Im_2	oPGHS-1-CN	Mb-N_3	oPGHS-1 (Fe^{2+})	HRP (Fe^{2+})	Mb (Fe^{2+})
	6chs	6chs	6chs	5chs	5chs	5chs	6cls	6cls	6cls	5chs	5chs	5chs
ν_2	1556	1565	1565	1571	1570	1566	1579	1583	1584	1558	1563	1563
ν_3	1483	1482	1484	1493	1487	1493	1502	1504	1506	1468	1472	1471
ν_4	1371	1373	1372	1370	1373	1371	1373	1373	1374	1358	1358	1356
ν_{10}			1611	1629	1626	1631	1640			1605	1605	1604
$\nu_{C=C}$	1622	1630	1621							1620	1625	1618
refs		*71*	*73*	*64,34*	*75*	*64*	*73*		*74*		*71*	*73*

[a] 6chs = six coordinate high-spin; 5chs = five coordinate high-spin; 6cls = six coordinate low-spin.

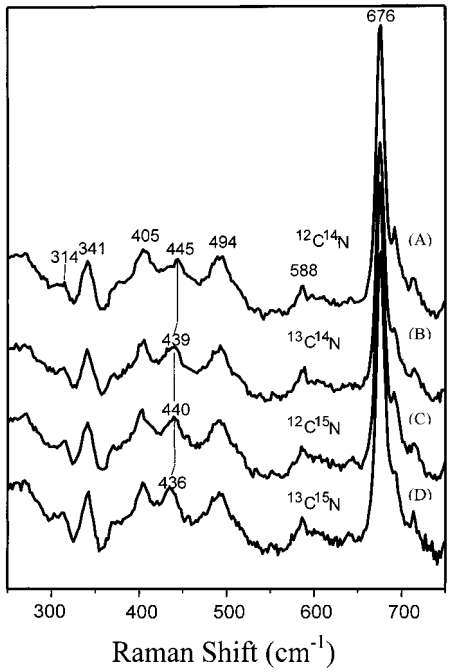

FIGURE 4: Low-frequency resonance Raman spectra of $^{12}C^{14}N$, $^{13}C^{14}N$, $^{12}C^{15}N$, and $^{13}C^{15}N$-oxidized unreconstituted oPGHS-1 adducts (A−D), respectively. The samples in 40 mM Tris-HCl at pH 7 with 0.1% $C_{10}E_7$ were incubated with the different cyanide isotopes at a final concentration of 10 mM. The conditions used for obtaining the low-frequency data were identical to those described for oxidized unreconstituted oPGHS-1 in the legend to Figure 3.

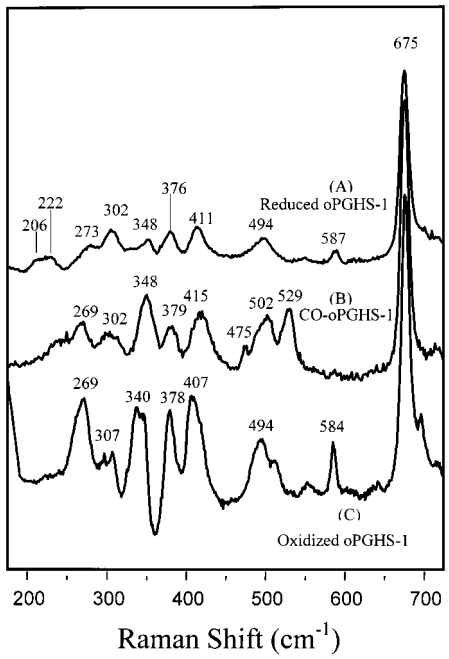

FIGURE 5: Low-frequency resonance Raman of oxidized and reduced oPGHS-1 and the CO-adduct of reduced oPGHS-1. Both the reduced A and B CO-adduct oPGHS-1 spectra were obtained with reconstituted enzyme while the oxidized form (C) was unreconstituted. The conditions for obtaining the low-frequency data were identical to those described for oPGHS-1 in the legend to Figure 3

structure (Table 1). The low-frequency spectrum of CN-oPGHS-1 contained a mode at 445 cm^{-1} which was sensitive to the mass of the cyanide ligand. This band shifted to approximately 440 cm^{-1} for $^{13}C^{14}N$ and $^{12}C^{15}N$ and to 436 cm^{-1} for $^{13}C^{15}N$ (Figure 4). There were no other isotope-sensitive bands in the spectra. This monotonic shift of the 445 cm^{-1} vibration to a lower frequency with increasing ligand mass is indicative of a ν[Fe−CN] stretch in an environment that allows cyanide to adopt a linear, unconstrained geometry (*45*). Similar observations of a lack of significant constraints on exogenous ligands by the distal environment were made by Gaspard et al. (*26*) for the CO-oPGHS-1 adduct.

Spectroscopic Characterization of Ferrous oPGHS-1. The optical absorption (Figure 2) and high-frequency Raman (Figure 3, λ_{ex} = 433 nm) spectra indicate that reduced oPGHS-1 exists as a high-spin, five-coordinate heme species (Table 1). We did not observe spectral evidence for the low-spin, six-coordinate ferrous oPGHS-1 species reported by Gaspard et al. (*26*). In contrast to our optical data in Figure 2, the UV−vis spectra of Gaspard et al. (*26*) contained absorption bands at 530 and 559 nm, that are characteristic of a low-spin ferrous species. Such optical absorption features, indicating a low-spin structure, have been observed upon generating an imidazole-ligated, reduced, or oxidized oPGHS-1 species (*26*, *44*).

The five-coordinate, high-spin, histidine-ligated heme in ferrous oPGHS-1 should exhibit an iron-histidine stretching vibration in the 200−260 cm^{-1} region, with its value reflecting the extent of anionic character present on the proximal histidine (*46*). For peroxidases with a strongly basic, histidinate ligand, the ν[Fe−His^-] mode occurs in the 240−260 cm^{-1} region (*46*, *47*). In globins and cytochrome *c* oxidases, in which the proximal ligand is a neutral histidine, this mode occurs between 200 and 230 cm^{-1} and is dependent on the extent of hydrogen bonding to the histidine N−H (*47*, *48*). The low-frequency spectrum of reduced oPGHS-1 (Figure 5) shows a doublet at 206 and 222 cm^{-1}; no modes are apparent in the region around 240 cm^{-1}. Consistent with its assignment as originating from Fe−His motion, the 206/222 cm^{-1} doublet is not present in spectra of oxidized oPGHS-1 nor of reduced oPGHS-1 incubated with CO (Figure 5). The doublet splitting in the Fe−His

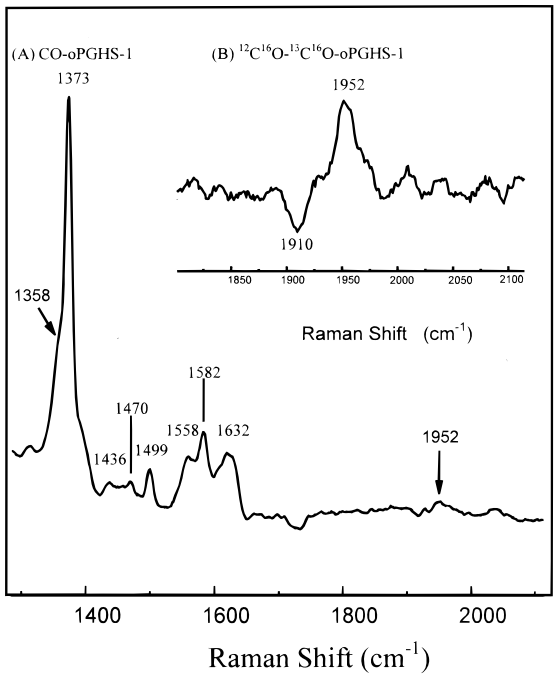

FIGURE 6: (A) High-frequency resonance Raman spectra of the natural abundance CO−adduct of reduced reconstituted oPGHS-1. The enzyme was reduced with dithionite and treated with $^{12}C^{16}O$ as described in Materials and Methods. The CO-oPGHS-1 adduct (32 μM) was in 50 mM potassium phosphate buffer, pH 7, and spectra were obtained at ~10 °C using the excitation line of 424 nm from the stilbene3 dye laser. The laser intensity was ≤1 mW. (B) Difference spectrum of the $^{12}C^{16}O-^{13}C^{16}O$ adducts of reconstituted oPGHS-1.

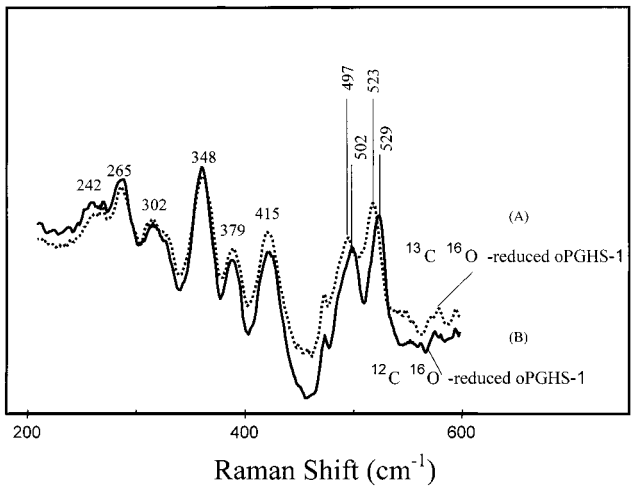

FIGURE 7: Low-frequency resonance Raman spectra of the (A) $^{13}C^{16}O$ and (B) $^{12}C^{16}O$ adducts of the reduced reconstituted CO-oPGHS-1. Samples were prepared and spectra were obtained as described in Materials and Methods and the legend to Figure 6.

vibration seen with oPGHS-1 has been observed previously both in peroxidases, with histidinate ligation [e.g., cytochrome *c* peroxidase (*33*, *47*)], and in oxidases, with histidine ligation [e.g., cytochrome *c* oxidase from bacilus subtilis (*49*) and thermus thermophilus (*50*)], as discussed below. The doublet character of the Fe−His vibration decreases the peak intensity of the Fe−His motion, which is most likely the reason that this mode escaped detection in earlier work (*26*).

CO Adduct of Ferrous oPGHS-1. The high-frequency Raman spectrum shows that CO, as expected, forms a low-spin, six-coordinate species with reduced oPGHS-1 as illustrated by the ν_4, ν_3, and ν_2 vibrations (Figure 6; Table 1). The shoulder at 1358 cm^{-1}, ν_4 from ferrous, high-spin oPGHS-1, illustrates that even at 1 mW incident power (or less), a small amount of photolysis of the CO-oPGHS-1 adduct occurs. Comparison of the low-frequency Raman spectra of the $^{12}C^{16}O$ and $^{13}C^{16}O$ derivatives of oPGHS-1 shows that two bands are sensitive to isotopic substitution (Figure 7). These bands occur at 529 and 502 cm^{-1}, in the natural abundance CO spectrum, and shift to 523 and 497 cm^{-1}, respectively, in the spectra of the adducts obtained with heavier forms of CO. The shifts of these bands are expected for a ν[Fe−CO] stretching vibration, as found for many CO-heme protein adducts (*51*−*53*.) and, accordingly, we assign these bands to two ν[Fe−CO] stretching modes. We observed no evidence of bending modes in the spectra. The 502 cm^{-1} band (Figure 7) is a mixture of the CO-bound species and the 494 cm^{-1} (Figure 5) porphyrin mode, visible in the oxidized, unligated, oPGHS-1 enzyme. It represents a smaller population of CO bound species than the 529 cm^{-1} mode.

The 529 cm^{-1} band has been previously reported as an ν[Fe−CO] stretching mode in oPGHS-1 by Gaspard et al. (*26*). Interestingly, however, they did not report a second ν[Fe−CO] stretching mode at 502 cm^{-1}. In addition to its small population, the 502 cm^{-1} Fe−CO conformer is more photolabile (data not shown) than the 529 cm^{-1} species and, as a consequence, it may go undetected if a high laser power is used. Under our experimental conditions, we minimized the amount of photolability, as indicated by the low intensity of ν_4 at 1358 cm^{-1}, by using laser powers of 1 mW or less.

In the high-frequency region of the Raman spectrum of reduced oPGHS-1 with natural abundance CO, a band at 1952 cm^{-1} shifts to 1910 cm^{-1} in the $^{13}C^{16}O$ spectrum (Figure 6). We assign this mode to a ν[CO] stretching vibration from the same species that gives rise to the 529 cm^{-1} v[Fe−CO] stretching mode, as both modes are highly populated and arise from the majority species. We did not detect any other ν[CO] stretching mode elsewhere in the spectrum. However, we do not discard the possibility of the existence of a second ν[CO] vibration, as found above for the ν[Fe−CO] stretching mode, since the high frequency mode has weak Raman intensity and the noise is considerable due to background fluorescence. We are presently setting up FTIR experiments to eliminate the fluorescence background and examine the high-frequency region for other CO vibrational bands of the CO-oPGHS-1 adduct.

Mutagenesis of Tyr504. As described above, a water molecule is located between and within hydrogen-bonding distance of both His388 and Tyr504 in oPGHS-1. Previous studies have shown that replacement of His388 with either a glutamine or an alanine leads to a catalytically inactive form of the enzyme but that these mutant enzymes retain their tertiary structures (*54*). To determine the importance of the putative hydrogen bond between water and Tyr504, we substituted Tyr504 with an alanine and determined the cyclooxygenase and peroxidase activities of the native oPGHS-1 and Y504A oPGHS-1 following their expression in COS-1 cells. Y504A oPGHS-1 retained 63% of the cyclooxygenase activity and 46% of the peroxidase activity of native oPGHS-1. Interestingly, two other mutants, Y504F oPGHS-1 and Y504Q oPGHS-1 lacked both peroxidase and

cyclooxygenase activity. Thus, perturbations of Tyr504 can lead to inactive mutant forms of the enzyme. However, the fact that the Y504A mutant retains substantial catalytic activity indicates that hydrogen bonding between Tyr504 and the water molecule located between His388 and Tyr504 is not necessary for oPGHS-1 to function.

DISCUSSION

The optical and Raman data for unreconstituted- and heme-reconstituted oPGHS-1 show that the spin and coordination state of the iron for both the oxidized and reduced states are independent of reconstitution, when the procedures described here are used. This is an important point as oPGHS-1 loses heme readily during isolation to yield a mixture of apo- and holo enzyme species. Thus, reconstitution is needed to improve the yield of active enzyme. For the resting, ferric enzyme, the ν_2 and ν_3 modes detected by Raman indicate an oxidized, six-coordinate, high-spin species (Table 1). This conclusion from the vibrational data is consistent with the optical data in which the charge-transfer band at 633 nm is characteristic of a six-coordinate state with water as the sixth ligand (*22*). There is no evidence of heterogeneity in either the spin or coordination state for the oxidized form of oPGHS-1.

The optical and vibrational data for resting oPGHS-1 differ from those exhibited by many wild-type plant peroxidases. For these species, the five-coordinate, high-spin or quantum mechanically mixed-spin ferric states usually dominate (*22*). The ligation differences between ferric oPGHS-1 and the plant peroxidases can be rationalized by our X-ray data, our observation that the proximal ligand in oPGHS-1 is a neutral histidine, and work by Sinclair et al. (*55*) that indicates that the position of the iron in the porphyrin plane is regulated by the strength of the iron-histidine bond. With relatively weak iron−proximal ligand interactions, the iron assumes an in-plane position, such that contact can be made with a water molecule on the distal side. This interaction produces the high-spin, six-coordinate structure, as seen with cytochrome *c* oxidases or met-myoglobin (*56*, *57*). Conversely, with stronger iron-proximal ligand interactions, the iron, even when oxidized, is forced out of the heme plane reducing its contact with distal ligands and thereby favoring a five-coordinate state. Peroxidases such as horseradish peroxidase or cytochrome *c* peroxidase contain a conserved aspartate-proximal histidine interaction that imparts histidinate character to the proximal histidine. This interaction produces a stronger proximal histidine−iron bond and favors the high-spin, five-coordinate structure observed in this class of peroxidases (*22*, *58*). Strong support for this interpretation has come from mutational studies in which the conserved aspartate in plant peroxidases has been replaced by non-hydrogen-bonding residues (*34*, *59*−*61*). In these mutants, the iron is now able to form the six-coordinate, high-spin species in the ferric state and the Fe−His vibration in the reduced state moves to much lower frequencies, indicating that the weakened iron-histidine interaction occurs in both valence states of the enzyme.

In the refined crystal structure of oPGHS-1, the proximal histidine is hydrogen bonded through a water molecule to an adjacent tyrosine (Figure 1). The His388-H_2O-Tyr504 interaction replaces the proximal histidine/aspartate interaction in the plant enzymes and produces a much weaker effect on the basicity of the H388 residue. As a consequence of the weak ligation between the heme iron and the proximal histidine, the ferric oPGHS-1 enzyme behaves analogously to the mutant peroxidases in terms of its ability to form the aquo-ligated, six-coordinate, high-spin ferric state. This observation is consistent with the low vibrational frequencies we obtained for the iron−histidine mode in the ferrous high-spin state and thus, indicates that the weak proximal effects which we observe for the oxidized enzyme persist upon reduction (see below).

Oxidized oPGHS-1 readily binds cyanide to form a low-spin, six-coordinate structure as indicated by the frequencies of the ν_2 (1583 cm^{-1}) and ν_3 (1504 cm^{-1}) core size markers. The low-spin structure shows an isotope sensitive mode at 445 cm^{-1}. This vibration shifts monotonically to lower frequency as the mass of the cyanide ligand is increased by isotopic substitution, which identifies it as the Fe−CN stretching vibration. Additional vibrational modes that exhibit a so-called zig−zag pattern upon isotopic substitution, which typifies an Fe−C═N bending vibration in a constrained pocket (*45*, *62***)** are absent in the Raman spectra. These results indicate a linear configuration for the cyanide ligand and are consistent with crystallographic data which indicate that the heme pocket is on the surface of the enzyme in an unencumbered environment and freely accessible to bulk water (*6*). In support of this conclusion, the Fe−CN stretching frequency of oPGHS-1 falls among the frequencies of cyanide adducts of HRP, Mb, and Hb, all of which show the Fe−CN stretching vibration near 450 cm^{-1} and have cyanide bound in a perpendicular, low-energy configuration (*45*, *63*).

Upon reduction, the heme of oPGHS-1 forms a ferrous, high-spin, five-coordinate state. This is shown by the valence and core-size markers ν_2 (1558 cm^{-1}), ν_3 (1468 cm^{-1}), ν_4 (1358 cm^{-1}), and ν_{10} (1605 cm^{-1}), all of which are indicative of this species. It has been suggested that reduced oPGHS-1 is unstable and quickly forms an alternative configuration with the ferrous iron in a six-coordinate, low-spin state with the distal histidine as the sixth ligand (*26*). Under our conditions, however, neither the optical absorption nor the resonance Raman spectra revealed the presence of a low-spin species. Taken together, the data for the resting, oxidized enzyme and for the reduced, unliganded species indicate homogeneous, well-defined structures.

In the low-frequency vibrational region of the reduced, unliganded enzyme, we observe the Fe−His vibration as a split band with apparent frequencies of 206 and 222 cm^{-1}. This is a clear demonstration that the histidine retains neutral character, consistent with the X-ray data of the oxidized oPGHS-1. A common property of the peroxidase class of enzymes is the presence of splitting in the Fe−His vibration, as observed for a variety of different peroxidases (*34*, *47*, *61*, *64*, *65*). This splitting is usually interpreted as arising from two different populations, one of which retains true histidinate character, the other of which remains as a histidine, but involved in a strong hydrogen bond with the aspartate residue in the immediate vicinity. For oPGHS-1, an analogous interpretation, but invoking neutral histidine either encumbered or unencumbered by a hydrogen bond, is likely. The refined crystal structure of oPGHS-1 indicates that H388 is capable of forming a hydrogen bond with the

water molecule that links it to Y504. If this hydrogen bond were to form, we would expect to see the Fe−His vibration near 220 cm^{-1}, whereas in the absence of the hydrogen bond, a lower frequency, near 205 cm^{-1}, is expected (*47*, *48*). The frequencies we observe, 206 and 222 cm^{-1}, are consistent with this analysis and indicate that the higher frequency mode arises from a population in which the hydrogen bond is intact, whereas the lower frequency vibration reflects a population of the enzyme in which the hydrogen bond is absent. We expect that there is a rapid interconversion between these two populations; time-resolved measurements to assess the dynamics of the process are planned. We also attempted to assess the accuracy of the interpretation above by fitting the spectrum in the 200−230 cm^{-1} frequency region to Gaussians in order to discriminate two separate populations versus a continuous distribution of substates. This analysis, however, did not allow an unambiguous distinction between the two possibilities. Nonetheless, we conclude that the low intensity and doublet nature of the ν[Fe−His] vibrations of oPGHS-1 result from different conformational states of the proximal histidine that reflect varying hydrogen-bonding interaction strengths.

The vibrational properties of the CO adduct of the reduced enzyme, reported here indicate that two ν[Fe−CO] stretching modes occur at 529 and 502 cm^{-1}, originating from two Fe−CO conformers as found in other peroxidases (*66*). The ν[Fe−CO] and ν[CO] stretching vibration values of 529 and 1952 cm^{-1}, are similar to those reported by Smulevich and co-workers (*65*) for cytochrome *c* peroxidase in which the aspartate in contact with the proximal histidine has been mutated. Her data, as discussed above, indicate that the proximal histidine is neutral in these mutants. The v[Fe−CO] and v[CO] frequencies reported by Smulevich and those we observe for CO-oPGHS-1 contrast sharply with those of most other peroxidases, which have values similar to imidazolate and thiolate models (*51*). Taken together, our results for the oxidized and the reduced enzyme, along with its adduct with CO, are consistent with the model that results from the X-ray refinement data of oPGHS-1. In all three states of the enzyme, the spectroscopic data are best interpreted as indicating an axial ligand behaving as a neutral histidine species. Thus, these data show that the character of the proximal ligand is insensitive to both valence and ligation changes at the iron and indicate that, in the reaction with peroxides, the proximal ligand most likely retains it histidine character.

In the classic push−pull reaction mechanism for histidine-ligated peroxidase catalysis (*17*, *18*) the distal histidine is postulated to act as a general base to accelerate the binding of the hydroperoxide by deprotonating the incoming substrate to generate the proposed Fe^{III}-OOR species. Subsequently, the same residue, acting as an acid, donates the proton to the terminal oxygen atom of the hydroperoxide. These distal pocket activities constitute the pull aspect of the mechanism. Concurrently, in the proximal pocket, an amino acid, usually an aspartate, hydrogen bonds to the proximal histidine and imparts significant anionic character to this residue. This hydrogen-bonding interaction, along with the location of the proximal histidine near the C-terminus of the proximal helix, increases the nucleophilicity of the histidine ligand, as indicated by the high frequency of the v[Fe−His] vibration, which is usually observed in the 240−250 cm^{-1} region (*65*, *67*−*69*). These proximal pocket activities constitute the push component of the mechanism. Taken together, the concerted push−pull process is thought to facilitate the heterolytic cleavage of the O−O molecule that generates compound I.

The evidence available continues to support the role postulated for the distal histidine in the push−pull mechanism, as mutations to this residue invariably decrease peroxidase activity precipitously, including that of PGHS (*54*, *70*). On the other hand, the importance of the push provided by a proximal histidine whose basicity can be significantly enhanced by local protein effects has been called into question (*19*, *23*, *24*).

The crystallographic, optical absorption, EPR, and resonance Raman data presented in this report add to the growing notion that a strong nucleophile in the proximal ligand position in heme peroxidases is not essential, as our data show that the proximal histidine of oPGHS-1 is not basic in character. This is consistent with the Y504A oPGHS-1 mutant which has peroxidase activity but lacks hydrogen bonding between it and the proximal histidine. In addition, the location of the proximal histidine near the C-terminus of its local helix, which has been invoked as increasing the electronegativity of the proximal ligand in plant peroxidases (*19*), appears to be muted in oPGHS-1 (*6*). Nevertheless, oPGHS-1 is an effective peroxidase despite its relatively weak proximal base and completes a two-electron reduction of substrate efficiently.

REFERENCES

1. Smith, W. L., and DeWitt, D. L. (1996) in *Advances in Immunology* (Dixon, F. J., Ed.) Vol. 62, pp 167−215, Academic Press, San Diego, CA.
2. Smith, W. L., Garavito, R. M., and DeWitt, D. L. (1996) *J. Biol. Chem. 271*, 33157−33160.
3. Marnett, L. J., Rowlinson, S. W., Goodwin, D. C., Kalgutkar, A. S., and Lanzo, C. A. (1999) *J. Biol. Chem. 274*, 22903−22906.
4. Smith, W. L., Garavito, R. M., and DeWitt, D. L. (2000) *Annu. Rev. Biochem*. (in press).
5. Marshall, P. J., and Kulmacz, R. J. (1988) *Arch. Biochem. Biophys. 266*, 162−170.
6. Picot, D., Loll, P. J., and Garavito, M. (1994) *Nature 367*, 243−249.
7. Kurumbail, R. G., Stevens, A. M., Gierse, J. K., McDonald, J. J., Stegeman, R. A., Pak, J. Y., Gildehaus, D., Miyashiro, J. M., Penning, T. D., Seibert, K., Isakson, P. C., and Stallings, W. C. (1996) *Nature 384*, 644−648.
8. Luong, C., Miler, A., Barnett, J., Chow, J., Ramesha, C., and Browner, M. F. (1996) *Nat. Struct. Biol. 3*, 927−933.
9. DeWitt, D. L. (1999) *Mol. Pharmacol. 55*, 625−631.
10. Marnett, L. J., and Kalgutkar, A. S. (1999) *Trends Pharmacol. Sci. 20*, 465−469.
11. Tsai, A., Wu, G., Palmer, G., Bambai, B., Koehn, J. A., Marshall, P. J., and Kulmacz, R. J. (1999) *J. Biol. Chem. 274*, 21695−21700.
12. Lambeir, A. M., Markey, C. M., Dunford, H. B., and Marnett, L. J. (1985) *J. Biol. Chem. 260*, 14894−14896.
13. Karthein, R., Dietz, R., Nastainczyk, W., and Ruf, H. H. (1988) *Eur. J. Biochem. 171*, 313−320.
14. Dietz, R., Nastainczyk, W., and Ruf, H. H. (1988) *Eur. J. Biochem. 171*, 321−328.
15. Koshkin, V., and Dunford, H. B. (1999) *Biochim. Biophys. Acta* 1430, 341−348.
16. Mizuno, K., Yamamoto, S., and Lands, W. E. M. (1982) *Prostaglandins 23*, 743−757.
17. Polulos, T. L. (1987) *Adv. Inorg. Biochem. 7*, 1.
18. Dawson, J. H. (1988) *Science 240*, 433−439.
19. Poulos, T. L. (1996) *J. Biol. Inorg. Chem. 1*, 356−359.

20. Choudhury, K., Sundaramoorthy, M., Hickman, A., Yonetani, T., Woehl, E., Dunn, M. F., Poulos, T. L. (1994) *J. Biol. Chem. 269*, 20239−20249.
21. Goodin, D. B. (1996) *J. Biol. Inorg. Chem. 1*, 360−363.
22. Smulevich, G. (1998) *Biospectroscopy 4* (5), 3−17.
23. Franzen, S., Roach, M. P., Chen, Y.-P., Dyer, B., Woodruff, W. H., and Dawson, J. H. (1998) *J. Am. Chem. Soc. 120*, 4658−4661.
24. Yi, X., Mroczko, M., Manoj, K., Wang, X., and Hager, L. (1999) *Proc. Natl. Acad. Sci. U.S.A. 96*, 12412−12417.
25. Kulmacz, R. J., Tsai, A. L., and Palmer, G. (1987) *J. Biol. Chem. 262*, 10524−10531.
26. Gaspard, S., Chottard, G., Mahy, J. P., and Mansuy, D. (1996) *Eur. J. Biochem. 238*, 529−537.
27. Harlan, J. E., Picot, D., Loll, P. J., and Garavito, R. M. (1995) *Anal. Biochem. 224* (2), 557−563.
28. Kulmacz, R. J., and Lands, W. E. M. (1987) in *Prostaglandins and Related Substances: A Practical Approach* (Benedetto, C., MacDonald-Gibson, R. G., Nigam, S., and Slater, T. E., eds) pp 209−227, IRL Press, Washington, D. C.
29. Otto, J. C., and Smith, W. L. (1994) *J. Biol. Chem. 269*, 19868−19875.
30. Spencer, A. G., Thuresson, E. A., Otto, J. C., Song, I., Smith, T., DeWitt, D. L., Garavito, R. M., and Smith, W. L. (1999) *J. Biol. Chem. 274*, 32936−32942.
31. Spencer, A. G., Woods, J. W., Arakawa, T., Singer, I. I., and Smith, W. L. (1998) *J. Biol. Chem. 273*, 9886−9893.
32. Rieke, C. J., Mulichak, A. M., Garavito, R. M., and Smith, W. L. (1999) *J. Biol. Chem. 274*, 17109−17114.
33. Finzel, B. C., Poulos, T. L., and Kraut, J. (1984) *J. Biol. Chem. 250*, 13027−13036.
34. Smulevich, G., Mauro, J. M., Fishel, L. A., English, A. M., Kraut, J., and Spiro, T. G. (1988) *Biochemistry 27*, 5477−5485.
35. Zeng, J., and Fenna, R. E. (1992) *Arch. Biochem. Biophys. 316*, 653−665.
36. Poulos, T. L., Edwards, S. L., Wariishi, H., and Gold, M. H. (1993) *J. Biol. Chem. 268*, 4429−4440.
37. Ferrer, J. C., Turano, P., Banci, L., Bertini, I., Morris, I. K., Smith, K. M., Smith, M., and Mauk, A. G. (1994) *Biochemistry 33*, 7819−7829.
38. Gajhede, J., Schuller, A., Henriksen, A., Smith, A. T., and Poulos (1997) *Nat. Struct. Biol. 4*, 1032−1038.
39. Van Der Ouderaa, F. J., Buytenhek, M., Slikkerveer, F. J., and Van Dorp, D. A. (1979) *Biochim. Biophys. Acta 572*, 29−42.
40. Kulmacz, R. J., and Lands, W. E. M. (1984) *J. Biol. Chem. 259*, 6358−6363.
41. Kulmacz, R. J., and Lands, W. E. M. (1987) in *Prostaglandins and related Substances: A Practical approach* (Benedetto, C., MacDonald-Gibson, R. G., Nigam, S., and Slater, T. E., Eds.) pp 209−227, IRL Press, Washington DC.
42. Hauksson, J. B., La Mar, G. N., Pande, U., Pandey, R. K., Parish, D. W., Singh, J. P., and Smith, K. M. (1990) *Biochim Biophys. Acta. 1041* (2), 94−186.
43. Deinum, G., Stone, J. R., Babcock, G. T., and Marletta, M. A. (1996) *Biochemistry 35*, 1540−1557.
44. Tsai, Ah-Lim., Kulmacz, R. J., Wang, J.-S., Wang, Y., Van Wart., H. E., and Palmer, G. (1993) *J. Biol. Chem. 268*, 8554−8563.
45. López-Garriga, J. J., Oertling, A., Kean, R. T., Hoogland, H., Wever, R., and Babcock, G. T. (1990) *Biochemistry 29*, 9387−9395.
46. Kitagawa, T. (1988) in *Biological Applications of Raman Spectroscopy* (Spiro, T. G., Ed.) Vol. 3, pp 97−131, Wiley Press, New York.
47. Smulevich G., Hu, S., Rodgers, K. R., Goodin, D. B., Smith, K. M., and Spiro, T. G. (1996) *Biospectroscopy 2*, 365−376.
48. Van Steelandt-Frentrup, J., Salmeen, I., and Babcock, G. T. (1981) *J. Am. Chem. Soc. 103*, 5981−5982.
49. Lauraeus, M., Wikstrom, M., Varotsis, C., Tecklenburg, M. J., and Babcock, G. T. (1992) *Biochemistry 31*, 10054−10060.
50. Oertling, W. A., Surerus, K. K., Einarsdottir, O., Fee, J. A., Dyer, B. R., and Woodruff, W. H. (1994) *Biochemistry 33*, 3128−3141.
51. Yu, N.-T., and Kerr, E. A. (1988) in *Biological Applications of Raman Spectroscopy* (Spiro, T. G., Ed.) Vol. 3, pp 39−93, Wiley Press, New York.
52. Ray, G. B., Li, X.-Y., Iberg, J. A., Sesseler, J. L., and Spiro, T. G. (1994) *J. Am. Chem. Soc. 116*, 162−176.
53. Wang, J., Stuehr, D., and Rousseau, D. (1997) *Biochemistry 36*, 4595−4606.
54. Shimokawa, T., and Smith, W. L. (1991) *J. Biol. Chem. 266*, 6168−6173.
55. Sinclair, R., Hallam, S., Chen, M., Chance, B., and Powers, L. (1996) *Biochemistry 35*, 15120−15128.
56. Babcock, G. T., Salmeen, I., Callahan, P., and Ondrias, M. (1981) *Biochemistry 20*, 959−966.
57. Sitter, A. J., Reczek, C. M., and Terner, J. (1985) *Biochim. Biophys. Acta. 828*, 229−235.
58. Mino, Y., Wariishi, H., Blackburn, N. J., Loehr, T. M., and Gold, M. H. (1988) *J. Biol. Chem. 263*, 7029−7036.
59. Smulevich, G., Wang, Y., Mauro, J. M., Wang, J., Fishel, L. A., Kraut, J., and Spiro, T. G. (1990) *Biochemistry 29*, 7174−7180.
60. Wang, J., Mauro, J. M., Edwards, S. L., Oatley, S. L., Fishel, L. A., Ashford, V. A., Xuong, N.-H., and Kraut, J. (1990) *Biochemistry 29*, 7160−7173.
61. Smulevich, G., Neri, F., Marzocchi, P., and Welinder, K. G. (1996) *Biochemistry 35*, 10576−10585.
62. Gersonde, K., Yu, N.-T., Ellen, K. A., Smith, K. M., and Parish, W. D. (1987) *J. Mol. Biol. 194*, 545−556.
63. Han, S., Madden, J. F., Siegel, L. M., and Spiro, T. G. (1989) *Biochemistry 28*, 5477−5485.
64. Nissum, M., Neri, F., Mandelman, D., Poulos, T. L., and Smulevich, G. (1998) *Biochemistry 37*, 8080−8087.
65. W.-J., Heldt, J., Smulevich, G., Feis, A., Focardi, C., Tams, J., and Welinder, G. K. (1994) *Biochemistry 33*, 15425−15432.
66. Smulevich, G., Mauro, J. M., Fishel, L. A., English, A. M., Kraut, J., and Spiro, T. (1988) *Biochemistry 27*, 5486−5492.
67. Smulevich, G., Dvangelista-Kirkup, R., English, A. M., and Spiro, T. G. (1986) *Biochemistry 25*, 4426−4430.
68. Hashimoto, S., Tatsuno, Y., and Kitagawa, T. (1986) *Proc. Natl. Acad. Sci. U.S.A. 83*, 2417−2421.
69. Goodin, D. B., and McRee, D. E. (1993) *Biochemistry 32*, 3313−3324.
70. Landino, L. M., Crews, B. C., Gierse, J. K., Hauser, D. D., and Marnett, L. J. (1997) *J. Biol. Chem. 272*, 21565−21574.
71. Rakshit, G., and Spiro, T. G. (1974) *Biochemistry 26*, 5317−5323.
72. Manthey, J. A., Boldt, N. J., Bocian, D. F., and Chan, S. I. (1986) *J. Biol. Chem. 261*, 6734−6741.
73. Choi, S., Spiro, T. G., Langry, K. G., Smith, K. M., Budd, D. L., and La Mar, G. N. (1982) *J. Am. Chem. Soc. 104*, 4345−4351.
74. Callahan, P. M., and Babcock, G. T. (1981) *Biochemistry 20*, 952−958.
75. Chuang Van Wart, H. E. (1989) *J. Biol. Chem. 264*, 14201−14215.

BI0002333